

Das, S. and Krebs, W.K. (2000). Sensor fusion of multi-spectral imagery. Institution of Electrical Engineers: Electronics Letters, 36, 1115-1116.

Sensor fusion of multi-spectral imagery

Sanjoy Das

Science Application International Corporation, Arlington, VA.

William K. Krebs

Department of Operations Research, Naval Postgraduate School, Monterey, CA.

In this article, we describe a new algorithm for the sensor fusion of imagery obtained at different bandwidths. The algorithm performs image fusion using a method based on principal components. We have demonstrated the effectiveness of the algorithm by applying it to fuse intensified CCD and infrared images.

Introduction

Images of the same scene obtained at different bandwidth are not always able to capture all details about the scene. They tend to incorporate differing, sometimes complementary, features, all of which are potentially useful to the viewer. It is often useful to produce a single composite image that is able to assimilate all these individual features.

Mere superposition of all input images does not produce good fused images. This is because, for n sensors, a feature that is visible through only a single input camera and not through the others, gets attenuated by a factor of n in the output image. Therefore a more elaborate scheme is necessary. A few algorithms for multispectral image fusion have been proposed. A method that is motivated largely by the vertebrate early visual system was developed recently [1, 2]. It can provide monochrome as well as color images. Another method that was proposed recently, simply superimposes images from different cameras as different colors in the fused image followed by color enhancement [3, 4].

This article proposes a new method of image fusion. The proposed algorithm performs gray level image fusion by examining the contrast of each input image and performing a weighted combination.

Outline of the Proposed Method

Consider n dimensional data in the form of m -vectors $\mathbf{x}_1, \mathbf{x}_2, \dots, \mathbf{x}_n$. In order to transform this data into a single m -vector \mathbf{y} , an n -vector \mathbf{q} is selected. The vector \mathbf{y} is then obtained as,

$$\mathbf{y}_q = [\mathbf{x}_1 \ \mathbf{x}_2 \ \dots \ \mathbf{x}_n] \cdot \mathbf{q}. \quad (1)$$

The subscript \mathbf{q} has been added to the \mathbf{y} to explicitly show its dependence on it. Let the variance of the single vector \mathbf{y} be denoted by $\sigma^2(\mathbf{y}_q)$. The (first) principal component is that n -vector \mathbf{p} along whose direction, the variance $\sigma^2(\mathbf{y}_p)$ is maximized, i.e. $\forall \mathbf{q}, \sigma^2(\mathbf{y}_p) \geq \sigma^2(\mathbf{y}_q)$. The principal component \mathbf{p} can easily be computed as the eigenvector of the correlation matrix $E[(\mathbf{x}-E(\mathbf{x}))(\mathbf{x}-E(\mathbf{x}))^T]$ having the largest eigenvalue. In what follows, we shall assume that there are two inputs - a low light visible image an infrared image. But the technique may be readily generalized for other types of images and for more than two inputs.

The fusion algorithm breaks up the entire images into smaller circular regions or 'partitions' and performs image fusion in a region-wise manner. Fusion is done based on the assumption that the variance of the image within any localized partition is a measure of the 'information' content of the partition. Henceforth, we shall treat an image as a two-dimensional array of pixels, and the pixel in the i^{th} row and the j^{th} column shall be

denoted by $\mathbf{I}(i, j)$. Using this notation, we define the $(p, q)^{\text{th}}$ partition of an image \mathbf{I} as follows,

$$\mathbf{R}_\mathbf{I}(p, q) = \{\mathbf{I}(i, j) | (p - i/\alpha)^2 + (q - j/\alpha)^2 < 1\}, \quad (2)$$

where α , an integer, is the region size. Clearly the indices p and q can acquire values in the range $[1, r/\alpha]$ and $[1, c/\alpha]$ respectively where $r \times c$ is the image size. It may be noted from the above equation that the regions are overlapping and that the partitioning process covers the entire image.

In order to determine the localized average pixel values in the images, the visible and infrared (IR) images, \mathbf{I}_{IR} and \mathbf{I}_{VIS} are smoothed by means of convolution with a Gaussian function. The smoothed images are given by (with the subscript X representing IR or VIS),

$$\mathbf{S}_\mathbf{X} = \mathbf{I}_\mathbf{X} \otimes \exp[-(x^2 + y^2)/\sigma^2] \quad (3)$$

where \otimes is the convolution operation. The width σ of the Gaussian function is closely related to the region size. The deviations from the smoothed images are computed as,

$$\mathbf{D}_\mathbf{X} = \mathbf{I}_\mathbf{X} - \mathbf{S}_\mathbf{X} \quad (4)$$

Next, the principal component of each partition \mathbf{R}_{DIR} and \mathbf{R}_{DVIS} of the arrays \mathbf{D}_{IR} and \mathbf{D}_{VIS} are computed. The $(p, q)^{\text{th}}$ principal component shall be denoted as $\mathbf{p}(p, q)$. Since the data is bivariate, \mathbf{p} shall have two components, \mathbf{p}_{IR} and \mathbf{p}_{VIS} . Within each partition, \mathbf{p} shall be appropriately biased towards the image with a higher information content. Therefore, performing a weighted combination of the IR and visible images using \mathbf{p} would lead to a fused image with a high information content. However, before this operation, an $r \times c$ array of weights \mathbf{W} has to be computed from \mathbf{p} . This is done in a straightforward manner by mapping the $r/\alpha \times c/\alpha$ of principal components to an $r \times c$ array of weights \mathbf{w}' and then convolving the resulting array with a Gaussian to ensure that the weights transition in a smooth manner to obtain the final weight arrays,

$$\mathbf{w}'_\mathbf{X}(i, j) = \mathbf{p}_\mathbf{X}(i/\alpha, j/\alpha), \quad (5)$$

and

$$\mathbf{w}_\mathbf{X} = \mathbf{w}'_\mathbf{X} \otimes \exp[-(x^2 + y^2)/\sigma^2] \quad (6)$$

Image fusion is carried out as the final step of the monochrome fusion process to obtain the fused monochrome image \mathbf{M} . This image is composed by averaging the smoothed input images and adding the weighted, normalized sum of the deviations.

$$\mathbf{M}(i, j) = [\mathbf{S}_{\text{IR}}(i, j) + \mathbf{S}_{\text{VIS}}(i, j)]/2 + [\mathbf{D}_{\text{IR}}(i, j) \cdot \mathbf{w}_{\text{IR}}(i, j) + \mathbf{D}_{\text{VIS}}(i, j) \cdot \mathbf{w}_{\text{VIS}}(i, j)] / [\mathbf{w}_{\text{IR}}(i, j) + \mathbf{w}_{\text{VIS}}(i, j)]. \quad (7)$$

In the above equation, the first term in the right hand side is the average of the smoothed IR and visible images. This provides the ‘background’ image to which the weighted deviations (the ‘information’) are added as the second term.

Results

We show examples of the performance of our proposed technique. In all the figures, the two rows correspond to images of two different scenes. The image sizes are 480×380, (after trimming 15 pixels from each edge) and $\alpha = 15$ and $\sigma = 5$ respectively. In Figure 1 are shown the low light visible (left) and the infrared (right) input images. The left images in Figure 2. are obtained by direct superposition,

$$\mathbf{M}_1 = [\mathbf{I}_{\text{IR}}(i,j) + \mathbf{I}_{\text{VIS}}(i,j)]/2. \quad (8)$$

In order to illustrate more directly the effect of using principal components, we also have provided in the right of Figure 2, the images that would be obtained if equal weights were assigned to the IR and visible inputs, i.e. if \mathbf{w}_{IR} and \mathbf{w}_{VIS} were identical,

$$\mathbf{M}_2 = [\mathbf{S}_{\text{IR}}(i,j) + \mathbf{S}_{\text{VIS}}(i,j)]/2 + [\mathbf{D}_{\text{IR}}(i,j) + \mathbf{D}_{\text{VIS}}(i,j)]/2. \quad (9)$$

\mathbf{M}_2 appears more contrast enhanced than the one obtained by superposition because adding the deviations to the smoothed image in Equation (7) has the equivalent effect of high-pass filtering the image. Figure 3 demonstrates the operation of the proposed method. The images on the left represent the normalized weight arrays that were computed. Darker regions are where the visible image is assigned more weight. The images to the right are the fused output image (\mathbf{M}) of Equation (7).

In addition to these images, a total of 20 images were fused using the proposed algorithm, and in all cases the result was satisfactory. At present, we are looking at a separate color processing stage to get suitably pseudo-colored images. We are also looking at enhancements to our technique for non-stationary imagery.

References

1. Waxman, A. M., Savoye E. D., Fay D. A., Aguilar M., Gove A. N., Carrick J. E. and Racamato J. P. Electronic Imaging Aids for Night Driving: Low Light CCD, Uncooled Thermal IR and Color Fused Visible/LWIR. *Proceedings of SPIE*, Vol. 2902 No. 2, 1997.
2. Waxman, A. M., Gove A. N., Fay D. A., Racamato J. P., Carrick J. E., Siebert M. A. and Savoye E. D. Color Night Vision: Opponent Processing in the Fusion of Visible and IR Imagery. *Neural Networks*, Vol. 10, No 1., 1997.

Das, S. and Krebs, W.K. (2000). Sensor fusion of multi-spectral imagery. Institution of Electrical Engineers: Electronics Letters, 36, 1115-1116.

3. Krebs, W. K., Scribner D. A., Miller G. M., Ogawa J. S. and Schuler J. Beyond Third Generation: A Sensor Fusion Targeting FLIR Pod for the F/A-18. *Proceedings of SPIE*, Vol. 3376, 1998.

4. Warren P., Scribner D., Schuler J., and Kruer M. Multi-Band Color Fusion. *Meeting of the IRIS Specialty Group on Passive Sensors*, March 1998.

Acknowledgements: The views expressed in this article are those of the authors and do not reflect the official policy or position of the Department of the Navy, Department of Defense, nor the United States Government.

Das, S. and Krebs, W.K. (2000). Sensor fusion of multi-spectral imagery. Institution of Electrical Engineers: Electronics Letters, 36, 1115-1116.

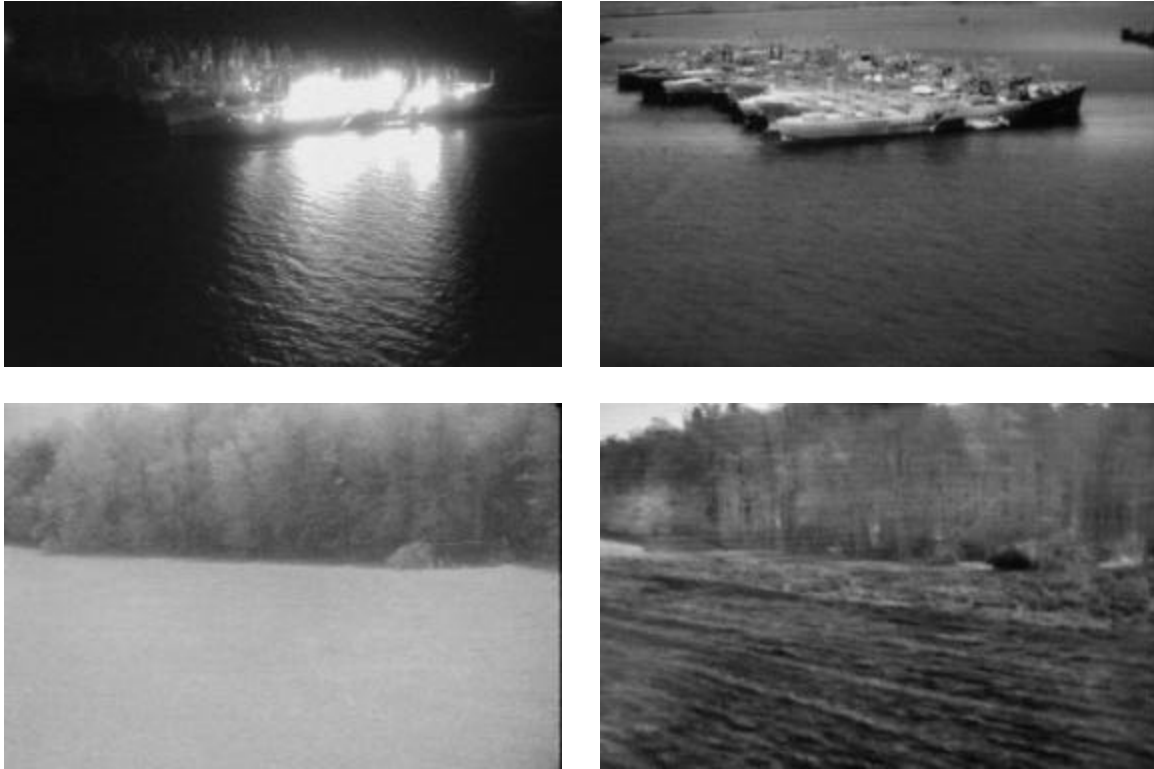


Figure 1. *The input visible and infrared images*

Das, S. and Krebs, W.K. (2000). Sensor fusion of multi-spectral imagery. Institution of Electrical Engineers: Electronics Letters, 36, 1115-1116.

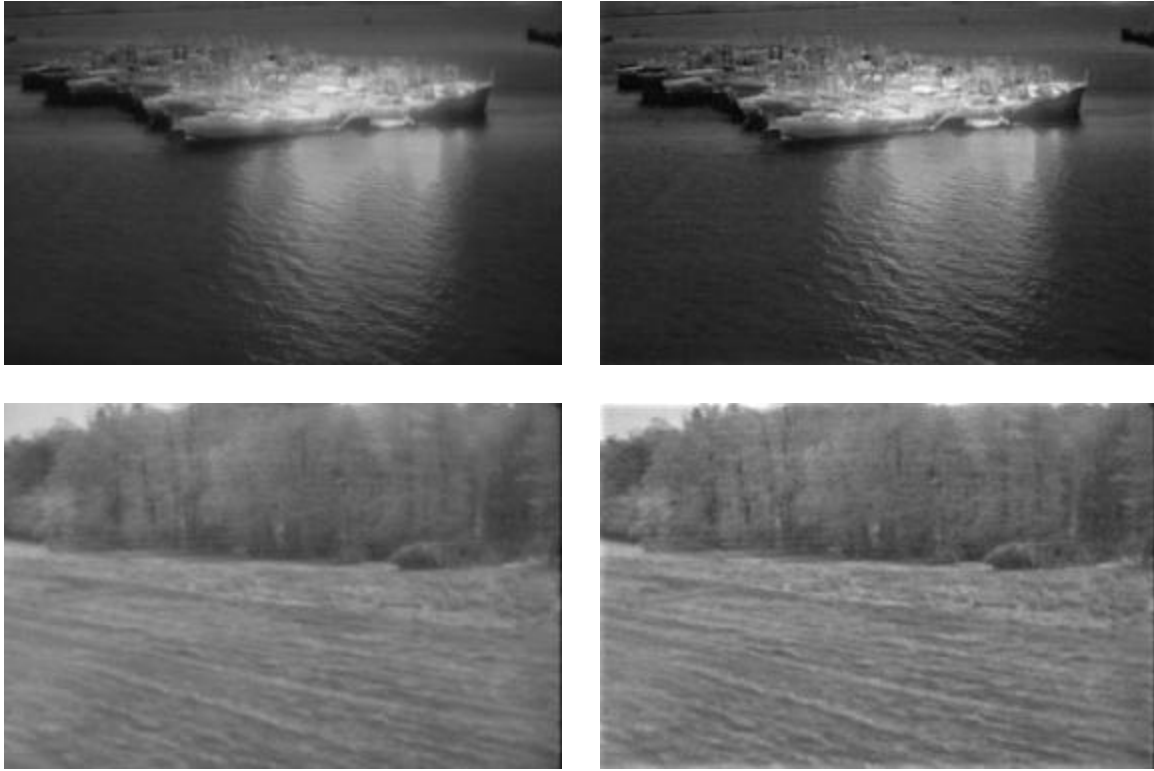


Figure 2. *The images obtained by Equations (8) and (9).*

Das, S. and Krebs, W.K. (2000). Sensor fusion of multi-spectral imagery. Institution of Electrical Engineers: Electronics Letters, 36, 1115-1116.

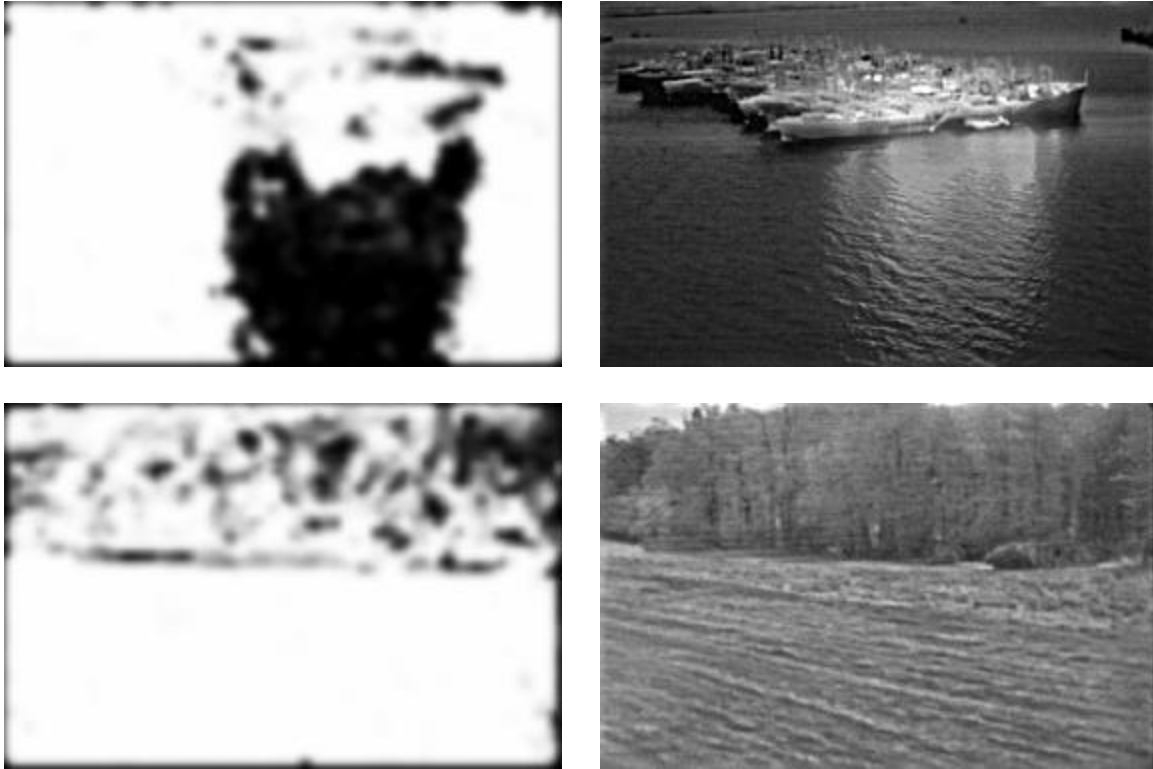


Figure 3. *The assigned weights and the image obtained as a result of image fusion in Equation (7).*